Numerical correction of optical vortex using a wrapped phase map analysis algorithm

Anne Margarette S. Maallo* and Percival F. Almoro

National Institute of Physics, University of the Philippines, Diliman, Quezon City 1101, Philippines
**Corresponding author: marge.maallo@gmail.com*

Received February 28, 2011; accepted March 4, 2011;
posted March 9, 2011 (Doc. ID 143334); published March 30, 2011

We demonstrate experimentally a technique for the numerical correction of an optical vortex with a unitary topological charge. A developed algorithm based on the axial behavior of a reconstructed wavefront is used in the detection of the optical vortex. Optimizations of the number of axial phase maps and the window size used in the algorithm yield the precise coordinates of the vortex eye. The obtained coordinates and vortex handedness are used in designing a proper filter, facilitating numerical correction of the vortex phase map. The developed algorithm can be applied to absolute phase and phase difference maps obtained through any reconstruction method. © 2011 Optical Society of America

OCIS codes: 050.4865, 070.7345, 120.2650, 090.1000, 100.5070, 090.1995.

In optical vortices, a light wave rotates around a singular point, creating dislocations that look like screws [1]. At the point of singularity or the vortex eye, the velocity of the rotation is infinite, resulting in an undefined phase and a vanishing intensity [1]. For a vortex with a unitary topological charge, the helical beam makes one twist within an axial distance of one wavelength [2]. The occurrence of phase singularities is generally regarded as optical noise, because it may degrade the performance of a coherent optical system. Like some discoveries in optics that belatedly found practical applications, optical vortices have recently been utilized in coherent metrology [3], optical twister manipulation [4], and optical vortex communication [5]. The characterization of vortices is therefore important, because it will facilitate active optical control, which paves the way for more applications, including, but not limited to, digital correction of optical noise. In [3], the detection of vortices was demonstrated using an algorithm based on a pixel neighborhood characterization. Numerical correction of geometric aberrations for accurate quantitative phase analysis requires the determination of the nature and extent of the aberrations present in the reconstructed phase maps, as demonstrated in digital holography [6] and phase retrieval [7]. When the aberration source is unknown, Zernike polynomial fitting is first carried out to determine the aberration functions [8]. These functions are used in constructing a filter phase map that will be subtracted from the experimental phase map. When the aberration source is known, direct subtraction of a theoretically generated filter phase map may be sufficient. To our knowledge, numerical phase correction has not yet been applied to optical vortices. On the one hand, Zernike polynomial fitting is difficult to implement for vortex phase maps due to the undefined phase at the singularity. Direct subtraction of a theoretically generated vortex filter, on the other hand, becomes a tedious task because the precise coordinates of the vortex eye remain obscured in the phase map noise. The task is virtually infeasible when compounded by the occurrence of multiple vortices, each having its own handedness and topological charge.

In this study, what we believe to be a novel algorithm for the characterization of obscured spatial features in retrieved phase maps is proposed. The algorithm is based on the axial behavior of reconstructed wavefronts. Experimental phase maps will be processed to demonstrate the validity of the proposed algorithm in obtaining the precise coordinates of an optical vortex, thus facilitating its numerical correction. Compared to [3], which used least-squares fitting, the proposed algorithm uses standard deviation (SD) as a quantifier of the pixels inside a window. Furthermore, the proposed algorithm is applied to reconstructed phase maps and not to intensity measurements [3]. Toward a proof-of-concept demonstration, a single vortex with a unitary topological charge is considered here. The influences of the algorithm window size and total number of planes in determination of the precise coordinates of the vortex eye and, subsequently, in the numerical correction of the optical vortex are investigated. The benefits of the vortex phase correction technique are error-free quantitative analyses of reconstructed wavefronts and, especially for the case of unwrapped phase maps, enhanced 3D phase visualization.

Figure 1 shows a schematic of the algorithm that makes use of the axial contrast of the SD values in phase maps to determine the location of the eye of an optical vortex. The algorithm starts with the propagation of a reconstructed wavefront to a region of interest where phase maps (dimensions, $N \times N$ pixels) are plotted at k axially displaced planes. The angular spectrum method of solving the Rayleigh–Sommerfeld wave propagation

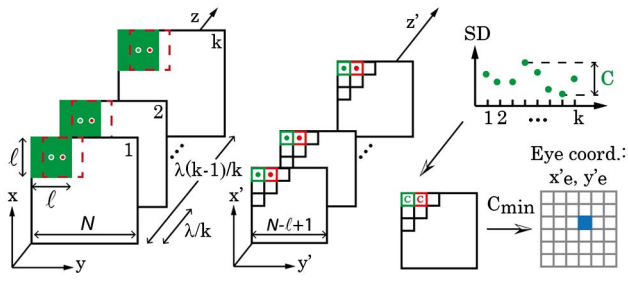

Fig. 1. (Color online) Schematic for determining the location of a vortex eye (transverse coordinates, x'_e and y'_e) using the contrast of SD values in the axial direction.

equation is used, because it maintains the same pixel size throughout the k axial planes [9,10]. The phase maps are depicted on the left side of Fig. 1. The distance between the first and the kth plane is $\lambda(k-1)/k$, where λ is the wavelength of the light source used. At a given plane, SD values for overlapping windows (solid green squares and red square broken lines—dimensions, $\ell \times \ell$ pixels) are calculated. After scanning the entirety of the phase map, a new array (dimension, $N - l + 1$) is formed, where each point (x', y') corresponds to a calculated SD value. These new axial arrays are depicted in the middle of Fig. 1. For the next step, the axial contrasts C of the SD values in the corresponding points throughout all the arrays are evaluated, yielding a single 2D contrast map. The contrast values are digitized for visualization. To locate the optical vortex, the digitization levels are correlated with the phase behavior in the transverse and axial directions. In a transverse plane, it is known that the vortex phase varies more rapidly toward the center compared to the outlying area. More pertinently, this behavior is approximately invariant throughout the axial planes; thus, the axial contrast of the SD values at the vortex eye is a minimum. This minimum value in the contrast map $C_{\min}$ is thereby used to locate the precise coordinates of the vortex eye, x'_e and y'_e.

Figure 2(a) shows a cropped section of the phase map containing an optical vortex with a unitary topological charge. The wavefront is a reconstruction of an ultraviolet laser beam ($\lambda = 405\,\text{nm}$) transmitted through a phase diffuser [7]. A local indentation on the diffuser surface introduced a phase change from 0 to 2π about the optical axis, thus generating the observed vortex. The wavefront is plotted ($N = 201$ pixels) at 16 axial planes within λ. The video file [Media 1, subpanel (a)] shows a sequence of the plotted axial phase maps. The screwlike twisting behavior of the vortex phase is evident as the wavefront advances over an axial distance within λ along the $-z$ direction. Figures 2(d)–2(f) (down the second column) depict the effects of the algorithm window size on the precise location of the vortex eye. To illustrate the optimization of the window size, we refer to $\ell = 21$, 13 and 5 pixels as oversized, optimum, and undersized window sizes, respectively. The grayscale display of the contrast maps has 16 levels. In the inset images, which have only two display levels (black or white), the white portions represent the lowest 16th level. When an oversized window is used [Fig. 2(d)], the detected vortex eye is a blob with a mean diameter of four pixels. In this case, the small uncertainty in the vortex coordinates may entail additional processing time before the phase correction can be carried out. An optimum window size results in a single minimum point (x'_e, y'_e) that corresponds to the vortex eye [Fig. 2(e)]. It is emphasized that such a precise set of vortex coordinates permits fast automated numerical vortex correction. When an undersized window is used [Fig. 2(f)], the artifacts that appear on the contrast map preclude further automated processing. Therefore, increasingly enhanced spatial features are revealed by the algorithm as the window size is decreased as far as the size at which artifacts appear. It is remarked that the choice for window size depends also on the intended application where specific spatial features need to be investigated. It is further remarked that the NA during optical recording still sets the maximum resolution of the system. An optimum statistical window size enhances only the detection of the spatial features on the phase maps. The window size (in pixels) is related to physical distances by multiplying the window size by the detector pixel size ($5.2\,\mu\text{m} \times 5.2\,\mu\text{m}$). Figures 2(g)–2(i) (down the third column) depict the effects of the total number of planes used in the algorithm. In Fig. 2(g) (with $k = 2$), the algorithm is not able to reveal any recognizable spatial features. An improvement is seen in Fig. 2(h), which is obtained when four phase maps are processed. However, this is evidently not an optimum number for k. Figure 2(i) (with $k = 8$) shows a distinct black dot corresponding to the vortex eye. Hence, with $k \geq 8$, the optical vortices are evidently located. A sequence of the contrast maps obtained for increasing total number of planes used is also shown in Media 1 [subpanel (b)]. To demonstrate the phase correction technique, a correction filter [Fig. 2(b)] is designed based on an equation for Bessel beams in combination with the obtained coordinates of the vortex eye. With the vortex eye already located, the handedness is investigated by sampling random points on the phase map in the periphery of the vortex eye. The particular vortex used is found to have a clockwise handedness. Figure 2(c) shows the result upon the subtraction of the vortex filter [Fig. 2(b)] from the cropped phase map ([Fig. 2(a)] dimension, 189 pixels = 201 – 13 + 1). The resultant phase map, which is that of a plane wave, is considered to be sufficiently corrected for the optical vortex. A video sequence of the advancing plane wavefront is shown in Media 1 subpanel (d). It is remarked that phase correction needs to be done only

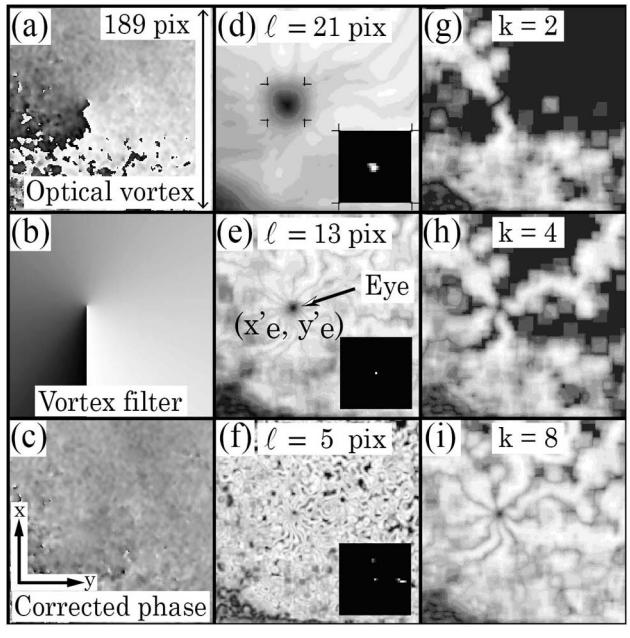

Fig. 2. (Media 1) Effects of the algorithm window size ℓ (second column) and the total number of planes k (third column) on the precise location of the vortex eye for the demonstration of the phase correction technique (first column). (a) Sample phase map. (b) Designed vortex filter with unitary topological charge, positive handedness and centered at (x'_e, y'_e). (c) Resulting corrected phase map upon subtraction of (b) from (a). Contrast maps for (d) $\ell = 21$, (e) $\ell = 13$, and (f) $\ell = 5$. Contrast maps for (g) $k = 2$, (h) 4, and (i) 8 planes.

once at a specific plane, because a corrected wavefront can be subsequently propagated to any plane of interest. It is also noted that the initial inclination of the vortex filter is not very critical and will result only in a relative phase shift. As an additional remark, the computational load highly depends on N, i.e., array size. As examples for computational loads, for $\ell = 13$, $k = 16$, and using a 1.8 GHz computer, $N = 301$, 201, and 101 pixels take respectively 90, 40, and 10 s to calculate the corresponding contrast maps. It is further remarked that the assumption of invariance of the vortex location within a wavelength range is valid only if the vortex is isolated and immune from the influences of other vortices. As a combination of noncoaxial vortices results in a field with richer vortex content [11], a possible extension of the technique to the case of multiple vortices would need to consider the influences of beam shapes, relative widths and amplitudes, and higher topological charges. From simulations, a vortex with a higher topological charge q will result in the periodic behavior of the phase map that repeats after every axial distance of λ/q. The multiple (q times) phase wrapping around the singularity seen in the transverse profile of the phase map leads to lower maximum contrast values, due to the more rapid phase changes. With the correct levels for displaying the contrast maps, however, the locations of such vortices are still resolvable with the algorithm.

Concluding, we have used a developed algorithm based on the axial behavior of retrieved phase maps to demonstrate a technique for the detection and correction of an optical vortex with unitary topological charge. Because of the optimized number of planes and window size in the algorithm, the coordinates of the vortex eye are precisely determined, thus facilitating the design of the proper correction filter. The proposed technique can be used for enhanced quantitative phase analysis and 3D phase visualization. The technique may be extended to the correction of multiple vortices that may have applications in the reduction of coherent optical noise. As a final remark, because the algorithm works on phase maps alone and no considerations are placed on the specific method used to generate such, the utilization of the algorithm is seen in a wide range of optical applications, including metrology, optical testing, phase microscopy, edge detection, 3D object localization, and tracking.

The authors acknowledge the Office of the Chancellor, in collaboration with the Office of the Vice-Chancellor for Research and Development, of the University of the Philippines Diliman for funding support through the Outright Research Grant. The authors also thank the Commission on Higher Education and the Department of Science and Technology, Philippine Council for Industry, Energy and Emerging Technology Research and Development for the financial support.

References

1. J. Nye and M. Berry, Proc. R. Soc. Lond. A **336**, 165 (1974).
2. D. Cojoc, B. Kaulich, A. Carpentiero, S. Cabrini, L. Businaro, and E. Di Fabrizio, Microelectron. Eng. **83**, 1360 (2006).
3. W. Wang, T. Yokozeki, R. Ishijima, M. Takeda, and S. Hanson, Opt. Express **14**, 10195 (2006).
4. V. R. Daria, D. Z. Palima, and J. Glückstad, Opt. Express **19**, 476 (2011).
5. Z. Wang, N. Zhang, and X.-C. Yuan, Opt. Express **19**, 482 (2011).
6. T. Colomb, F. Montfort, J. Kühn, N. Aspert, E. Cuche, A. Marian, F. Charrière, S. Bourquin, P. Marquet, and C. Depeursinge, J. Opt. Soc. Am. A **23**, 3177 (2006).
7. P. F. Almoro, P. N. Gundu, and S. G. Hanson, Opt. Lett. **34**, 521 (2009).
8. D. Malacara, *Optical Shop Testing* (Wiley, 2007).
9. P. Ferraro, S. De Nicola, G. Coppola, A. Finizio, D. Alfieri, and G. Pierattini, Opt. Lett. **29**, 854 (2004).
10. F. Zhang, I. Yamaguchi, and L. Yaroslavsky, Opt. Lett. **29**, 1668 (2004).
11. G. Molina-Terriza, J. Recolons, and L. Torner, Opt. Lett. **25**, 1135 (2000).